Investigating the Impact of Asymptomatic Carriers on COVID-19 Transmission

Jacob B. Aguilar,[1] Juan B. Gutierrez,[2*]

[1]Department of Mathematics and Sciences, Saint Leo University,
Saint Leo, FL 33574, USA
[2]Department of Mathematics, University of Texas at San Antonio,
San Antonio, TX 78249, USA

[*]To whom correspondence should be addressed; E-mail: juan.gutierrez3@utsa.edu.

Coronavirus disease 2019 (COVID-19) is a novel human respiratory disease caused by the SARS-CoV-2 virus. Asymptomatic individuals in the context of COVID-19 are those subjects who are carriers of the virus but display no clinical symptoms. Current evidence reveals that this sub-population is a major contributing factor in the propagation of this disease, while escaping detection by public health surveillance systems. In this manuscript, we present a mathematical model taking into account asymptomatic carriers. Our results indicate a basic reproduction number as high as 26.5. The first three weeks of the model exhibit exponential growth, which is in agreement with average case data collected from thirteen countries with universal health care and robust communicable disease surveillance systems; the average rate of growth in the number of reported cases is 25% per day during this period. The model was

applied to every county in the US to give estimates of mild, severe, and critical case severity, and also mortality. These estimates can be considered an upper bound.

1 Background

Coronavirus disease 2019 (COVID-19) is a novel human respiratory disease caused by the SARS-CoV-2 virus. The first cases of COVID-19 infections surfaced in December 2019 in Wuhan city, the capital of Hubei province. Shortly after, the virus quickly spread to several countries (*1*). On January 30, 2020 The World Health Organization (WHO) declared the virus as a public health emergency of an international scope (*2*). Twelve days later, on March 11, 2020 it was officially declared to be a global pandemic.

A fundamental difference concerning the COVID-19 pandemic compared to the SARS-CoV 2003 epidemic is that substantial transmission is possible with mild to no symptoms. Asymptomatic transmission in populations has been documented (*3,4*). Furthermore, the viral loads of asymptomatic carriers are very similar to those of the symptomatic (*5*). A recent study concluded that asymptomatic and symptomatic carriers may have the same level of infectiousness (*6*). This fact results in COVID-19 being more difficult to control than SARS-CoV. These findings demand a reassessment of the transmission dynamics of the COVID-19 outbreak accounting for the asymptomatic sub-population.

The primary goal of this manuscript is to characterize the epidemiological dynamics of COVID-19 via a compartmentalized model in which an asymptomatic sub-population is considered. The most notable result is that with the most recent data at the time of publication, COVID-19 has a large basic reproductive number, $\mathcal{R}_0$, estimated at a mean value of 26.5.

2 Methods

In this section we summarize the main results, and leave mathematical proofs for the appendix. Numerical estimates for the basic reproduction number follow.

2.1 Mathematical Model

The formulation of the $SEYAR$ model for the spread of COVID-19 begins with decomposing the total host population (N) into the following five epidemiological classes: susceptible human (S), exposed human (E), symptomatic human (Y), asymptomatic human (A), and recovered human (R).

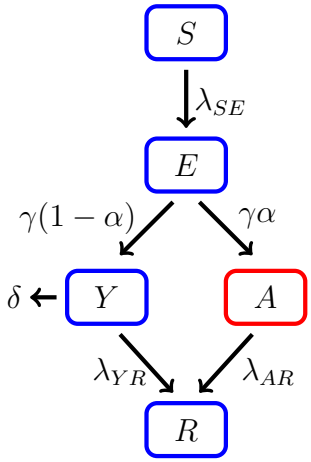

Figure 1: Schematic diagram of a COVID-19 model including an asymptomatic compartment. The solid lines represent progression from one compartment to the next. Humans progress through each compartment subject to the rates described below.

Listed below is a $SEYAR$ dynamical system (1) describing the dynamics of COVID-19 transmission in a closed human population.

$$\begin{cases} \dot{S} = -\left(\beta_Y \frac{Y}{N} + \beta_A \frac{A}{N}\right) S, \\ \dot{E} = \left(\beta_Y \frac{Y}{N} + \beta_A \frac{A}{N}\right) S - \gamma E, \\ \dot{Y} = \gamma(1-\alpha)E - (\delta + \lambda_{YR})\, Y, \\ \dot{A} = \gamma\alpha E - \lambda_{AR} A, \\ \dot{R} = \lambda_{AR} A + \lambda_{YR} Y, \end{cases} \tag{1}$$

where, $N = S + E + Y + A + R$. It is worth mentioning that for a basic $SEIR$ model, where there is only one infected compartment, the progression rate from the susceptible to the exposed class λ_{SE} is equal to the product of the effective contact rate β and the proportion of infected individuals $\frac{I}{N}$, so that

$$\lambda_{SE} = \beta \frac{I}{N}.$$

In our model, we decompose the infected compartment into symptomatic and asymptomatic sub-compartments. Due to this decomposition, the progression rate is given by the weighted sum

$$\lambda_{SE} = \left(\beta_Y \frac{Y}{N} + \beta_A \frac{A}{N} \right).$$

The reproduction number $\mathcal{R}_0$ provides a way to measure the contagiousness of the disease in question. It serves as an indicator of the overall strength of an epidemic and is utilized by public health authorities to gauge the severity of an outbreak. The design and effective implementation of various intervention strategies are guided by estimates of $\mathcal{R}_0$. Established outbreaks will fade provided that interventions maintain $\mathcal{R}_0 < 1$.

2.2 Computation of $\mathcal{R}_0$

During the first stages of an epidemic, calculating $\mathcal{R}_0$ poses significant challenges. Evidence of this difficulty was observed in the 2009 influenza A (H1N1) virus pandemic (*7*). Particularly, the COVID-19 pandemic has a different characterization in each country in which it has spread due to differences in surveillance capabilities of public health systems, socioeconomic factors, and environmental conditions.

During the initial growth of an epidemic, Anderson et al. (*8*) derived the following formula to determine $\mathcal{R}_0$:

$$\mathcal{R}_0 = 1 + \frac{D \ln 2}{t_d}, \tag{2}$$

where D is the duration of the infectious period, and t_d is the initial doubling time. To find t_d, simply solve for t in $Y = a \cdot (1 + r)^t$, where $Y = 2a$, and $r = 24.5\%$ (the rationale for this number is explained below). Thus, $t_d = \ln 2 / \ln b$. Using the values reported on Table 1, the calculated value of the basic reproduction number using Equation 2 is $\mathcal{R}_0 = 11$, which is substantially larger than what is being reported in the literature as the COVID-19 pandemic unfolds, but should be understood as an underestimation of the true $\mathcal{R}_0$ because there is no consideration of asymptomatic carriers in the model of Anderson et al. (*8*).

A striking characteristic of COVID-19 is the nearly perfect exponential growth reported during the first three weeks of community transmission. Figure 2 shows the number of cases reported in thirteen countries with universal health care and strong surveillance systems as of March 17, 2020. Ten of these countries are in the European zone, plus Australia, Canada and Japan. An exponential fitting for each country reveals an average coefficient of determination $r^2 = 0.9846 \pm 0.0164$. The average growth rate r in the exponential model $Y = a \cdot (1 + r)^t$, where t is time measured in days, is $r = 24.5\%$, and the average of the initial conditions is $a = 96$ cases.

Thus, the average growth of the symptomatic compartment (Y) of COVID-19 during the first three weeks of community transmission is characterized in average by the equation

$$Y = 96 \cdot 1.245^t. \tag{3}$$

The estimate on Equation 2 was adjusted to transform the initial average symptomatic population $Y_0 = 96$ into a percentage population, using the the time series of reported cases in Figure 2, and taking a to be the ratio between the medians of the minimum and maximum number of cases in the thirteen countries selected for this study, as of March 16^{th}, 2020. The exponential function for the population growth of COVID-19

Table 1: Model Parameters

Parameter	Description	Dimension	Value	Source
β_A	effective contact rate from asymptomatic to susceptible	$days^{-1}$	1.12	(*9*)
β_Y	effective contact rate from symptomatic to susceptible	$days^{-1}$	0.62	(*9*)
γ^{-1}	mean incubation period	days	5.1	(*10*)
α	probability of becoming asymptomatic upon infection transition rate	n/a	0.86	(*9*)
λ_{AR}^{-1}	mean asymptomatic infectious period	$days^{-1}$	0.05	(*11*)
λ_{YR}^{-1}	mean symptomatic infectious period	$days^{-1}$	0.027	(*12*)
δ	disease-induced death rate	days	$0.032(1-\alpha)$	(*13*)
λ_{AY}	asymptomatic to symptomatic	$days^{-1}$	0	Assumed
λ_{RS}	relapse rate	$days^{-1}$	0	Assumed
Λ	human recruitment rate	humans $\times$ $days^{-1}$	0	Assumed
ξ	natural mortality rate	$days^{-1}$	0	Assumed

symptomatic cases, in terms of percentage of a population, is:

$$\begin{aligned} Y =& \frac{median(\min(Y_d))}{median(\max(Y_d))} \cdot 1.245^t, \\ =& 0.0693 \cdot 1.245^t, \end{aligned} \tag{4}$$

where Y_d represents the distribution of time series of reported cases, and t is time measured in days.

There are well known challenges in attempting to fit an exponential function to epidemiological data (*14–16*). However, given the relatively slow progression of COVID-19, and the protracted incubation period, the growth of the symptomatic population can be well characterized by an exponential function for up to three weeks.

Given an age pyramid for a community, it is possible to compute estimates for the expected number of clinical cases. The Chinese Center for Disease Control (CCDC) reported on February 11^{th}, 2020, the results obtained from the analysis of data from the

first wave of COVID-19 in Wuhan (*17*). The probabilities of developing mild, severe, and critical conditions, as well as the probability of death were computed for all age groups. The CCDC uses increments of ten years to define each age group. In the US, the United States Bureau of the Census (USBOC) uses increment of five years to define age groups. Thus, we assumed a constant distribution of the probabilities deported by the CCDC as they were mapped to the more granular age groups defined by the USBOC.

The model was applied to every county in the US to give estimates of mild, severe, and critical case severity, and also mortality. These results are presented in the supplemental material. The source of data for the number of cases was ourworldindata.org (*18*). Data about US population was obtained from the USBOC.

3 Results

Disease-Free Equilibrium (DFE) points are solutions of a dynamical system corresponding to the case where no disease is present in the population. Define the diseased classes to be E, Y, A, so that

$$\mathbf{w}^\star = \left(\frac{\Omega}{\xi}, 0, 0, 0, 0\right)^T.$$

In a mathematical context, the reproduction number $\mathcal{R}_0$ is a threshold value that characterizes the local asymptotic stability of the underlying dynamical system at a DFE. The reproduction number arising from the dynamical system (1) is given by

$$\mathcal{R}_0 = \frac{\beta_Y(1-\alpha)}{\lambda_{YR}+\delta} + \frac{\alpha\beta_A}{\lambda_{AR}}. \tag{5}$$

A verification of the calculation yielding the reproduction number $\mathcal{R}_0$ given by equation (5) is provided in the electronic supplementary material.

Figure 3 shows a calculation of the SEYAR model using the parameters reported in Table 1. This representation of the progression of the disease must be understood as a

theoretical development; in reality, the progression of an epidemic depends on a multitude of factors that necessarily result in deviations from this ideal case.

The size of the COVID-19 reproduction number documented in the literature is relatively small. Our estimates indicate that $\mathcal{R}_0 = 26.5$, in the case that the asymptomatic sub-population is accounted for. In this scenario, the peek of symptomatic infections is reached in 36 days with approximately 9.5% of the entire population showing symptoms, as shown in Figure 3.

4 Discussion

The time series of symptomatic individuals provided by the SEYAR model can inform the likely progression of the disease. The compartment Y must be considered as an upper bound for the progression of the COVID-19 pandemic, that is, what surveillance systems could observe in absence of public health interventions and behavior modification. However, as the COVID-19 pandemic evolves, governments around the world are taking drastic steps to limit community spread. This will necessarily dampen the growth of the disease, and the dynamical system proposed in this study will cease to have any practical utility as is. Nevertheless, it has captured faithfully the first stages of the pandemic, and remains a stark reminder of what the cost of inaction could be.

The SEYAR model is useful to compute $\mathcal{R}_0$. It is unlikely that a pathogen that blankets the planet in three months can have a basic reproduction number in the vicinity of 3, as it has been reported in the literature (*19–24*). SARS-CoV-2 is probably among the most contagious pathogens known. Unlike the SARS-CoV epidemic in 2003 (*25*), where only symptomatic individuals were capable of transmitting the disease. Asymptomatic carriers of the COVID-19 virus are most likely capable of transmission to the same degree as symptomatic. In a public health context, the silent threat posed by the presence of

asymptomatic carriers in the population results in the COVID-19 pandemic being much more difficult to control.

The reproduction number $\mathcal{R}_0$ shown in Equation 5 arising from our model admits a natural biological interpretation. To guide this discussion, it is pertinent to refer to the original epidemic model proposed by W. O. Kermack and A. G. McKendrick in 1927 (*26*), see Figure 5 below, has the corresponding dynamical system

$$\begin{cases} \dot{S} = -\beta \frac{I}{N} S, \\ \dot{I} = \beta \frac{I}{N} S - \omega I, \\ \dot{R} = \omega I. \end{cases} \tag{6}$$

Epidemiologically speaking, the basic reproduction number is the average number of secondary infections generated by a single infection in a completely susceptible population. It is proportional to the product of infection/contact (a), contact/time (b) and time/infection (c). The quantity a is the infection probability between susceptible and infectious individuals, b is the mean contact rate between susceptible and infectious individuals and c is the mean duration of the infectious period.

The case of an increasing infected sub-population corresponds to the occurrence of an epidemic. This happens provided that $\dot{I} = \beta \frac{I}{N} S - \omega I > 0$ or $\frac{\beta}{\omega} \frac{S}{N} > 1$. Under the assumption that in the beginning of an epidemic, virtually the total population is susceptible, that is $\frac{S}{N} \approx 1$. As a result, we arrive at the following equivalent condition

$$\mathcal{R}_0 := \frac{\beta}{\omega} > 1.$$

The parameter β in Figure 5 is equal to ab and ω is equal to c^{-1}. This combination of parameters stands to reason as it is a ratio of the effective contact rate β and the mean infectious period ω^{-1}.

Since the disease-induced death rate $\delta \approx 0$, the reproduction number (5) for our model has a similar natural interpretation as the average of the effective contact rates

β_Y, β_A and mean infectious periods λ_{YR}^{-1}, λ_{AR}^{-1} for the symptomatic and asymptomatic sub-populations, weighted with the probability of becoming asymptomatic upon infection α.

This study shows that the population of individuals with asymptomatic COVID-19 infections are driving the growth of the pandemic. The value of $\mathcal{R}_0$ we calculated is nearly one order of magnitude larger than the estimates that have been communicated in the literature up to this point in the development of the pandemic.

A Appendix

Listed below is the generalized *SEYAR* dynamical system (7) which falls into the class of models covered in (*27*), see Figure 6.

$$\begin{cases} \dot{S} = \Lambda + \lambda_{RS} R - \left(\beta_Y \frac{Y}{N} + \beta_A \frac{A}{N} + \xi\right) S, \\ \dot{E} = \left(\beta_Y \frac{Y}{N} + \beta_A \frac{A}{N}\right) S - (\gamma + \xi) E, \\ \dot{Y} = \gamma(1-\alpha) E - (\xi + \delta + \lambda_{YR}) Y + \lambda_{AY} A, \\ \dot{A} = \gamma\alpha E - (\lambda_{AR} + \lambda_{AY} + \xi) A, \\ \dot{R} = \lambda_{AR} A + \lambda_{YR} Y - (\lambda_{RS} + \xi) R, \end{cases} \tag{7}$$

where, $N = S + E + Y + A + R$.

Lemma 1. *(Reproduction Number for the SEYAR COVID-19 Model). Define the following quantity*

$$\mathcal{R}_0 := \frac{\gamma}{\gamma + \xi} \left(\frac{\beta_Y}{\delta + \lambda_{YR} + \xi} \left(\frac{\alpha \lambda_{AY}}{\lambda_{AR} + \lambda_{AY} + \xi} - (\alpha - 1) \right) + \frac{\alpha \beta_A}{\lambda_{AR} + \lambda_{AY} + \xi} \right). \tag{8}$$

Then, the DFE $\mathbf{w}^\star$ *for the SEYAR model (7) is locally asymptotically stable provided that* $\mathcal{R}_0 < 1$ *and unstable if* $\mathcal{R}_0 > 1$.

Proof. Firstly, we order the compartments so that the first four correspond to the infected sub-populations and denote $\mathbf{w} = (E, Y, A, R, S)^T$. The corresponding DFE is

$$\mathbf{w}^{\star} = \left(0, 0, 0, 0, \frac{\Omega}{\xi}\right)^{T}.$$

Utilizing the next generation method developed by Van den Driessche and Watmough (*28*), system (7) is rewritten in the following form

$$\dot{\mathbf{w}} = \Phi(\mathbf{w}) = \mathcal{F}(\mathbf{w}) - \mathcal{V}(\mathbf{w}),$$

where $\mathcal{F} := (\mathcal{F}_1, \ldots, \mathcal{F}_5)^T$ and $\mathcal{V} := (\mathcal{V}_1, \ldots, \mathcal{V}_5)^T$, or more explicitly

$$\begin{pmatrix} \dot{E} \\ \dot{Y} \\ \dot{A} \\ \dot{R} \\ \dot{S} \end{pmatrix} = \begin{pmatrix} \left(\beta_Y \frac{Y}{N} + \beta_A \frac{A}{N}\right) S \\ 0 \\ 0 \\ 0 \\ 0 \end{pmatrix} - \begin{pmatrix} (\gamma + \xi) E \\ -\gamma(1-\alpha) E + (\xi + \delta + \lambda_{YR}) Y - \lambda_{AY} A \\ -\gamma\alpha E + (\lambda_{AR} + \lambda_{AY} + \xi) A \\ -\lambda_{AR} A - \lambda_{YR} Y + (\lambda_{RS} + \xi) R \\ -\Lambda - \lambda_{RS} R + \left(\beta_Y \frac{Y}{N} + \beta_A \frac{A}{N} + \xi\right) S \end{pmatrix}.$$

The matrix $\mathcal{V}$ admits the decomposition $\mathcal{V} = \mathcal{V}^- - \mathcal{V}^+$, where the component-wise definition is inherited. In a biological context, $\mathcal{F}_i$ is the rate of appearance of new infections in compartment i, $\mathcal{V}_i^+$ stands for the rate of transfer of individuals into compartment i by any other means and $\mathcal{V}_i^-$ is the rate of transfer of individuals out of compartment i. Now, let F and V be the following sub-matrices of the Jacobian of the above system, evaluated at the solution $\mathbf{w}^{\star}$

$$F = \left(\frac{\partial \mathcal{F}_i}{\partial x_j}\Big|_{\mathbf{w}^{\star}}\right)_{1 \le i,j \le 3} = \begin{pmatrix} 0 & \beta_Y & \beta_A \\ 0 & 0 & 0 \\ 0 & 0 & 0 \end{pmatrix}$$

and

$$V = \left(\frac{\partial \mathcal{V}_i}{\partial x_j}\Big|_{\mathbf{w}^{\star}}\right)_{1 \le i,j \le 3} = \begin{pmatrix} (\gamma + \xi) & 0 & 0 \\ \gamma(\alpha - 1) & (\xi + \delta + \lambda_{YR}) & -\lambda_{AY} \\ -\gamma\alpha & 0 & (\lambda_{AR} + \lambda_{AY} + \xi) \end{pmatrix}.$$

A direct calculation shows that

$$V^{-1} = \begin{pmatrix} (\gamma+\xi)^{-1} & 0 & 0 \\ -\frac{\gamma((\alpha-1)(\lambda_{AR}+\xi)-\lambda_{AY})}{(\gamma+\xi)(\xi+\delta+\lambda_{YR})(\xi+\lambda_{AY}+\lambda_{AR})} & (\xi+\delta+\lambda_{YR})^{-1} & \lambda_{AY}\left((\xi+\delta+\lambda_{YR})\left(\xi+\lambda_{AY}+\lambda_{AR}\right)\right)^{-1} \\ \gamma\alpha\left((\gamma+\xi)\left(\lambda_{AR}+\lambda_{AY}+\xi\right)\right)^{-1} & 0 & (\lambda_{AR}+\lambda_{AY}+\xi)^{-1} \end{pmatrix}$$

and FV^{-1} is given by the following matrix

$$\begin{pmatrix} \frac{\gamma}{(\gamma+\xi)(\lambda_{AR}+\lambda_{AY}+\xi)}\left(-\frac{\beta_Y((\alpha-1)(\lambda_{AR}+\xi)-\lambda_{AY})}{\delta+\lambda_{YR}+\xi}+\beta_A\alpha\right) & \beta_Y\left(\delta+\lambda_{YR}+\xi\right)^{-1} & \frac{1}{\lambda_{AR}+\lambda_{AY}+\xi}\left(\frac{\beta_Y\lambda_{AY}}{\delta+\lambda_{YR}+\xi}+\beta_A\right) \\ 0 & 0 & 0 \\ 0 & 0 & 0 \end{pmatrix}.$$

Let $\mathcal{I}$ denote the 3×3 identity matrix, so that the characteristic polynomial $P(\lambda)$ of the matrix FV^{-1} is given by

$$\begin{aligned} P(\lambda) &= \det\left(FV^{-1}-\lambda\mathcal{I}\right), \\ &= \lambda^2\left(\lambda-\left(\frac{\gamma\beta_Y}{(\gamma+\xi)(\delta+\lambda_{YR}+\xi)}\left(\frac{\alpha\lambda_{AY}}{\lambda_{AR}+\lambda_{AY}+\xi}+1-\alpha\right)+\frac{\gamma\alpha\beta_A}{(\gamma+\xi)(\lambda_{AR}+\lambda_{AY}+\xi)}\right)\right). \end{aligned}$$

The solution set $\{\lambda_i\}_{1\le i\le 3}$ is given by

$$\left\{0,0,\frac{\gamma\beta_Y}{(\gamma+\xi)(\delta+\lambda_{YR}+\xi)}\left(\frac{\alpha\lambda_{AY}}{\lambda_{AR}+\lambda_{AY}+\xi}+1-\alpha\right)+\frac{\gamma\alpha\beta_A}{(\gamma+\xi)(\lambda_{AR}+\lambda_{AY}+\xi)}\right\}.$$

Therefore, the reproduction number for the $SEYAR$ model (7) is given by

$$\begin{aligned} \mathcal{R}_0 &:= \rho\left(FV^{-1}\right), \\ &= \max_{1\le i\le 3}\{\lambda_i\}, \\ &= \frac{\gamma\beta_Y}{(\gamma+\xi)(\delta+\lambda_{YR}+\xi)}\left(\frac{\alpha\lambda_{AY}}{\lambda_{AR}+\lambda_{AY}+\xi}+1-\alpha\right)+\frac{\gamma\alpha\beta_A}{(\gamma+\xi)(\lambda_{AR}+\lambda_{AY}+\xi)}, \\ &= \frac{\gamma}{\gamma+\xi}\left(\frac{\beta_Y}{\delta+\lambda_{YR}+\xi}\left(\frac{\alpha\lambda_{AY}}{\lambda_{AR}+\lambda_{AY}+\xi}-(\alpha-1)\right)+\frac{\alpha\beta_A}{\lambda_{AR}+\lambda_{AY}+\xi}\right). \end{aligned}$$

The proof of the lemma regarding the local asymptotic stability of the DFE $\mathbf{w}^\star$ corresponding to the *SEYAR* Model (7) is now complete after invoking Theorem 2 in (*28*). □

A verification of the calculation yielding the reproduction number $\mathcal{R}_0$ given by equation (8) is provided in the electronic supplementary material.

References

1. W.-j. Guan, *et al.*, *New England Journal of Medicine* (2020).

2. World Health Organization, Coronavirus disease (covid-19) outbreak.

3. K. Mizumoto, K. Kagaya, A. Zarebski, G. Chowell, *medRxiv* (2020).

4. Z. Hu, *et al.*, *Science China Life Sciences* pp. 1–6 (2020).

5. L. Zou, *et al.*, *New England Journal of Medicine* (2020).

6. C. R. MacIntyre, *Global Biosecurity* **1** (2020).

7. H. Nishiura, G. Chowell, M. Safan, C. Castillo-Chavez, *Theoretical Biology and Medical Modelling* **7**, 1 (2010).

8. R. Anderson, G. Medley, R. May, A. Johnson, *Mathematical Medicine and Biology: a Journal of the IMA* **3**, 229 (1986).

9. R. Li, *et al.*, *medRxiv* (2020).

10. S. A. Lauer, *et al.*, *Annals of Internal Medicine* .

11. F. Zhou, *et al.* (2020).

12. K. McIntosh, M. S. Hirsch, A. Bloom .

13. D. Baud, *et al.*, *The Lancet Infectious Diseases* (2020).

14. G. Chowell, C. Viboud, *Infectious disease modelling* **1**, 71 (2016).

15. G. Chowell, L. Sattenspiel, S. Bansal, C. Viboud, *Physics of life reviews* **18**, 114 (2016).

16. G. Chowell, C. Viboud, L. Simonsen, S. M. Moghadas, *Journal of The Royal Society Interface* **13**, 20160659 (2016).

17. V. Surveillances, *China CDC Weekly* **2**, 113 (2020).

18. H. R. Max Roser, E. Ortiz-Ospina, *Our World in Data* (2020). Https://ourworldindata.org/coronavirus.

19. J. M. Read, J. R. Bridgen, D. A. Cummings, A. Ho, C. P. Jewell, *medRxiv* (2020).

20. T. Liu, *et al.* (2020).

21. M. Majumder, K. D. Mandl, *China (January 23, 2020)* (2020).

22. Z. Cao, *et al.*, *medRxiv* (2020).

23. S. Zhao, *et al.*, *International Journal of Infectious Diseases* **92**, 214 (2020).

24. N. Imai, *et al.*, *Reference Source* (2020).

25. R. M. Anderson, *et al.*, *Philosophical Transactions of the Royal Society of London. Series B: Biological Sciences* **359**, 1091 (2004).

26. W. Kermack, A. Mckendrick, *Proc Roy Soc London* **A 115**, 700 (1927).

27. J. B. Aguilar, J. B. Gutierrez, *Bulletin of Mathematical Biology* **82**, 42 (2020).

28. P. Van den Driessche, J. Watmough, *Mathematical biosciences* **180**, 29 (2002).

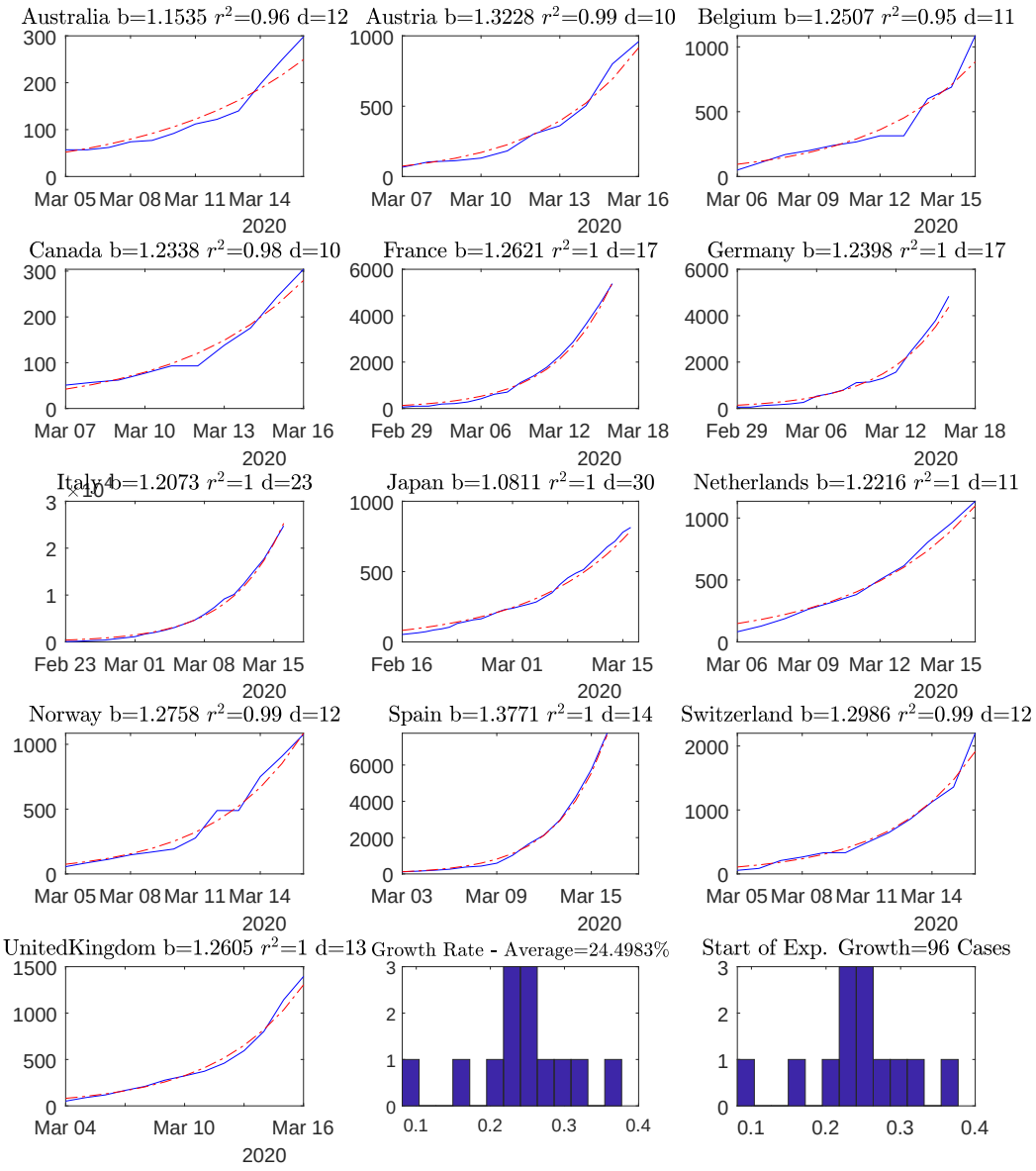

Figure 2: Thirteen countries with less than three weeks of data for COVID-19 cases and strong surveillance systems for communicable diseases.

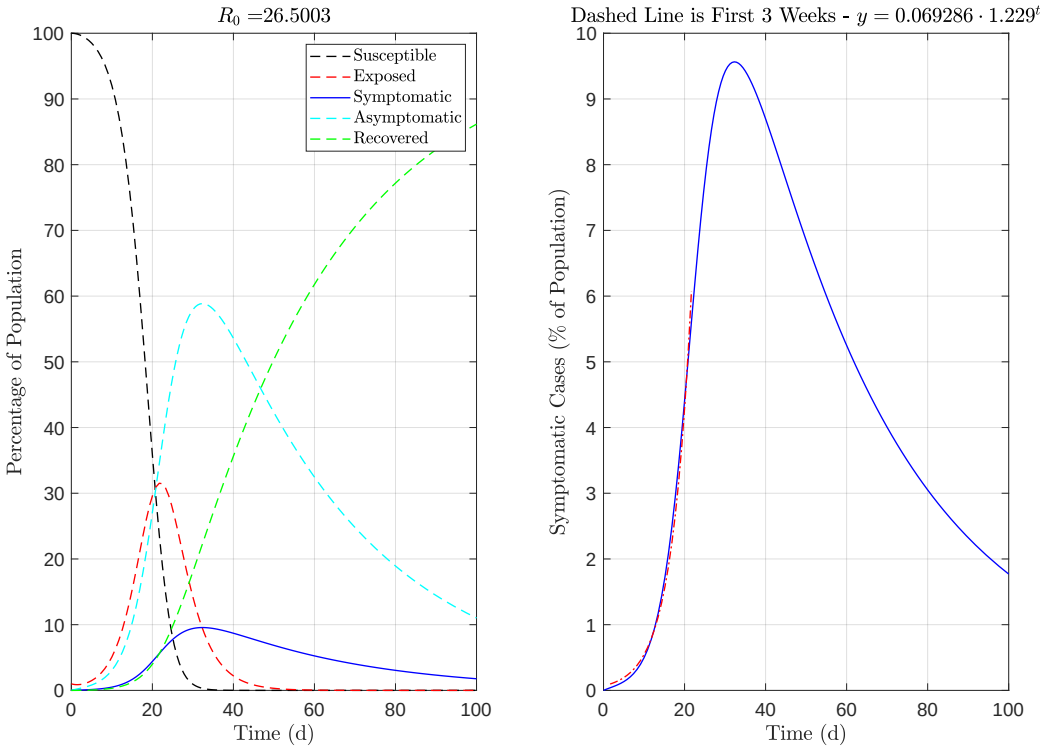

Figure 3: Numerical implementation of a SEYAR model with the parameters listed on Table 1. The right-hand panel shows the time series for the symptomatic compartment, with an exponential function fitted to match the first three weeks of the outbreak.

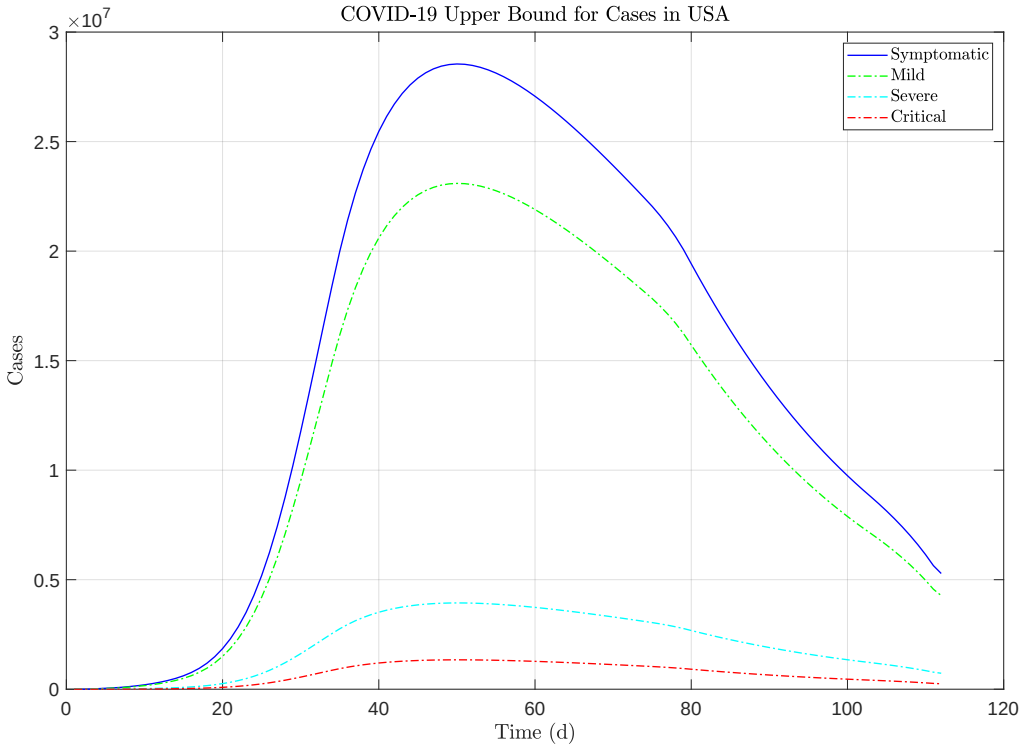

Figure 4: Projected number of cases in the US.

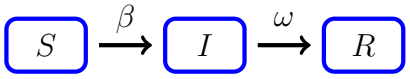

Figure 5: This figure is a schematic diagram of a SIR model consisted of three compartments, namely: susceptible (S), infected (I) and recovered (R). Humans progress through each compartment subject to the rates described above.

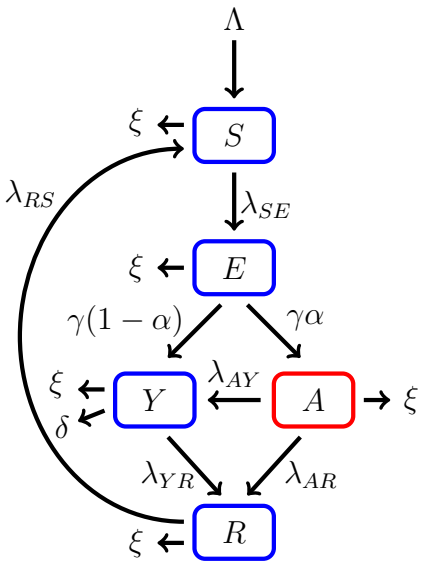

Figure 6: This figure is a schematic diagram of a generalized COVID-19 model including an asymptomatic compartment. The solid lines represent progression from one compartment to the next. Humans enter the susceptible compartment either through birth of migration and then progress through each additional compartment subject to the rates described above.

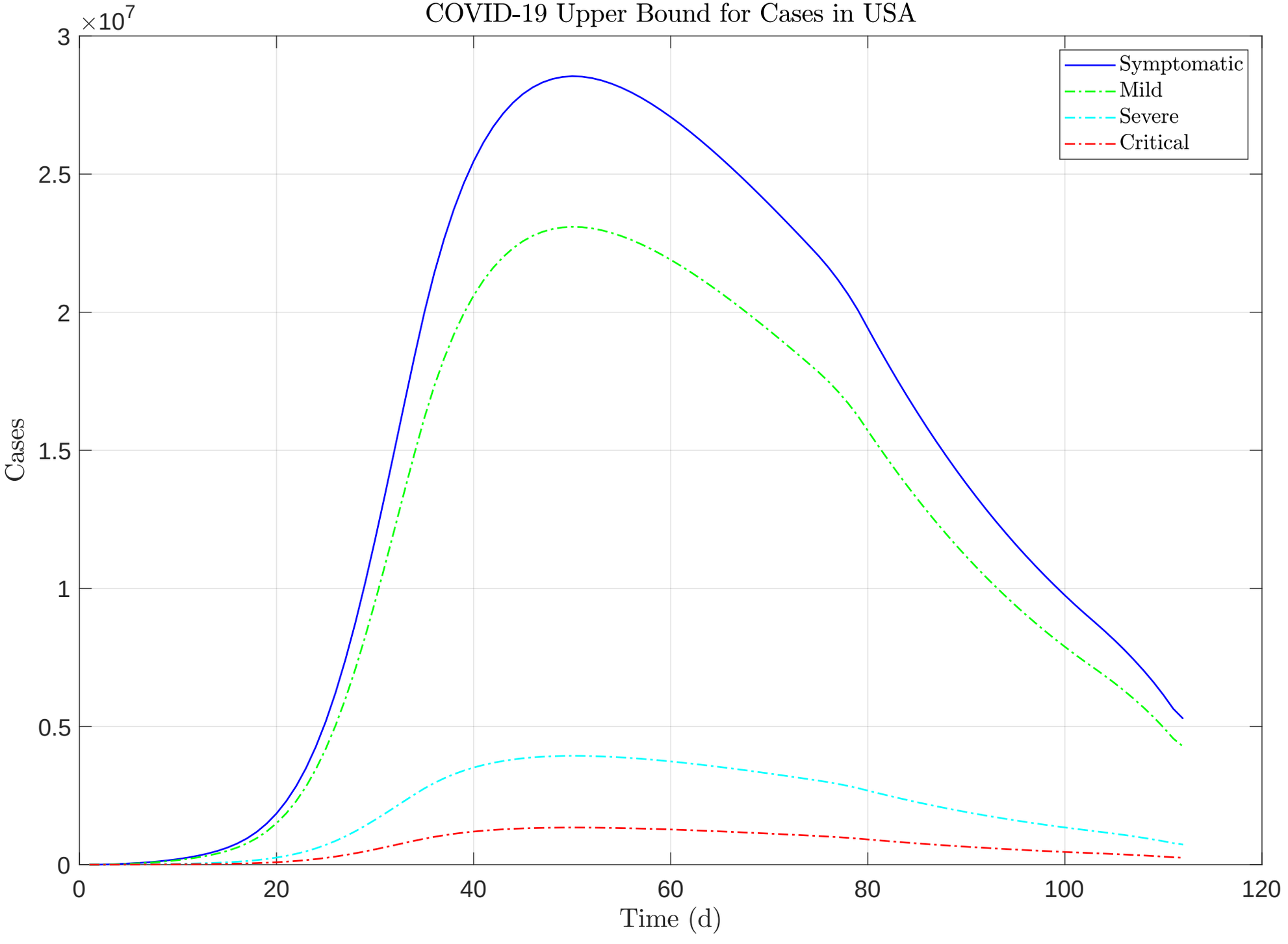
COVID-19 Upper Bound for Cases in USA
×10^7
3
2.5
2
1.5
1
0.5
0
Cases
0
20
40
60
80
100
120
Time (d)
Symptomatic
Mild
Severe
Critical

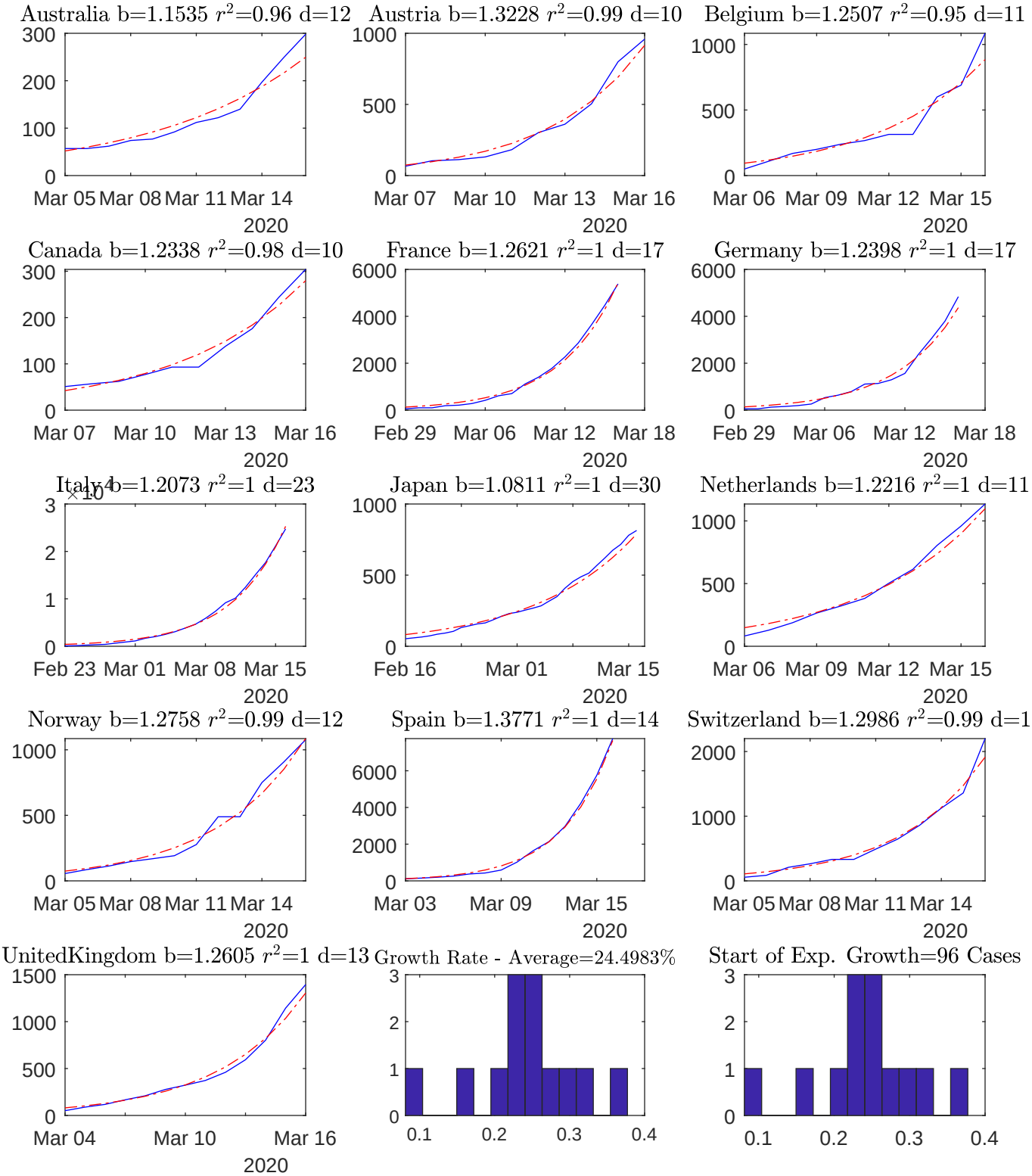
Australia b=1.1535 r^2=0.96 d=12
Austria b=1.3228 r^2=0.99 d=10
Belgium b=1.2507 r^2=0.95 d=11
Canada b=1.2338 r^2=0.98 d=10
France b=1.2621 r^2=1 d=17
Germany b=1.2398 r^2=1 d=17
Italy b=1.2073 r^2=1 d=23
×10^4
Japan b=1.0811 r^2=1 d=30
Netherlands b=1.2216 r^2=1 d=11
Norway b=1.2758 r^2=0.99 d=12
Spain b=1.3771 r^2=1 d=14
Switzerland b=1.2986 r^2=0.99 d=12
UnitedKingdom b=1.2605 r^2=1 d=13
Growth Rate - Average=24.4983%
Start of Exp. Growth=96 Cases
2020

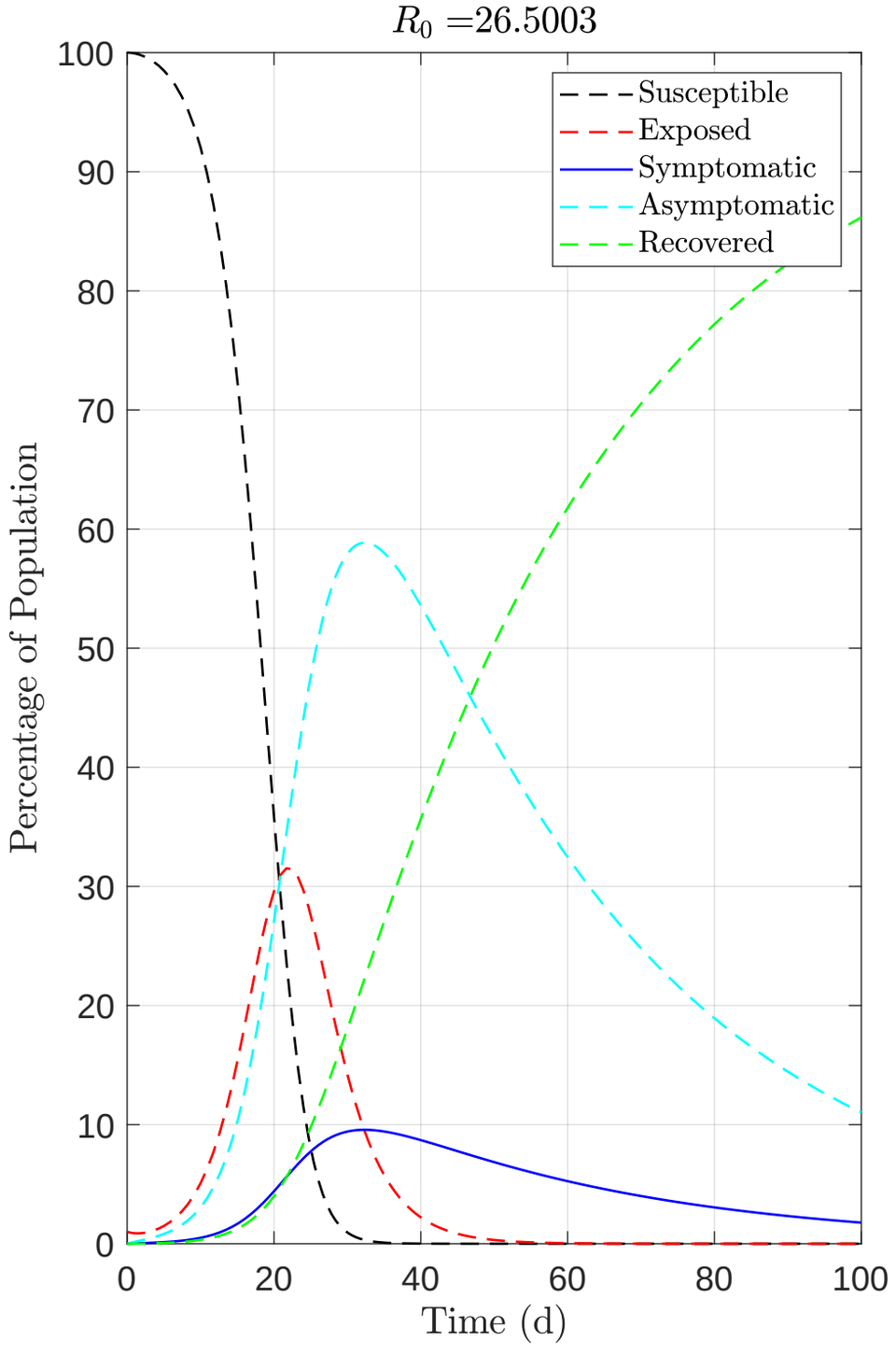
R_0 =26.5003
Susceptible
Exposed
Symptomatic
Asymptomatic
Recovered
Percentage of Population
Time (d)
0
10
20
30
40
50
60
70
80
90
100
0
20
40
60
80
100

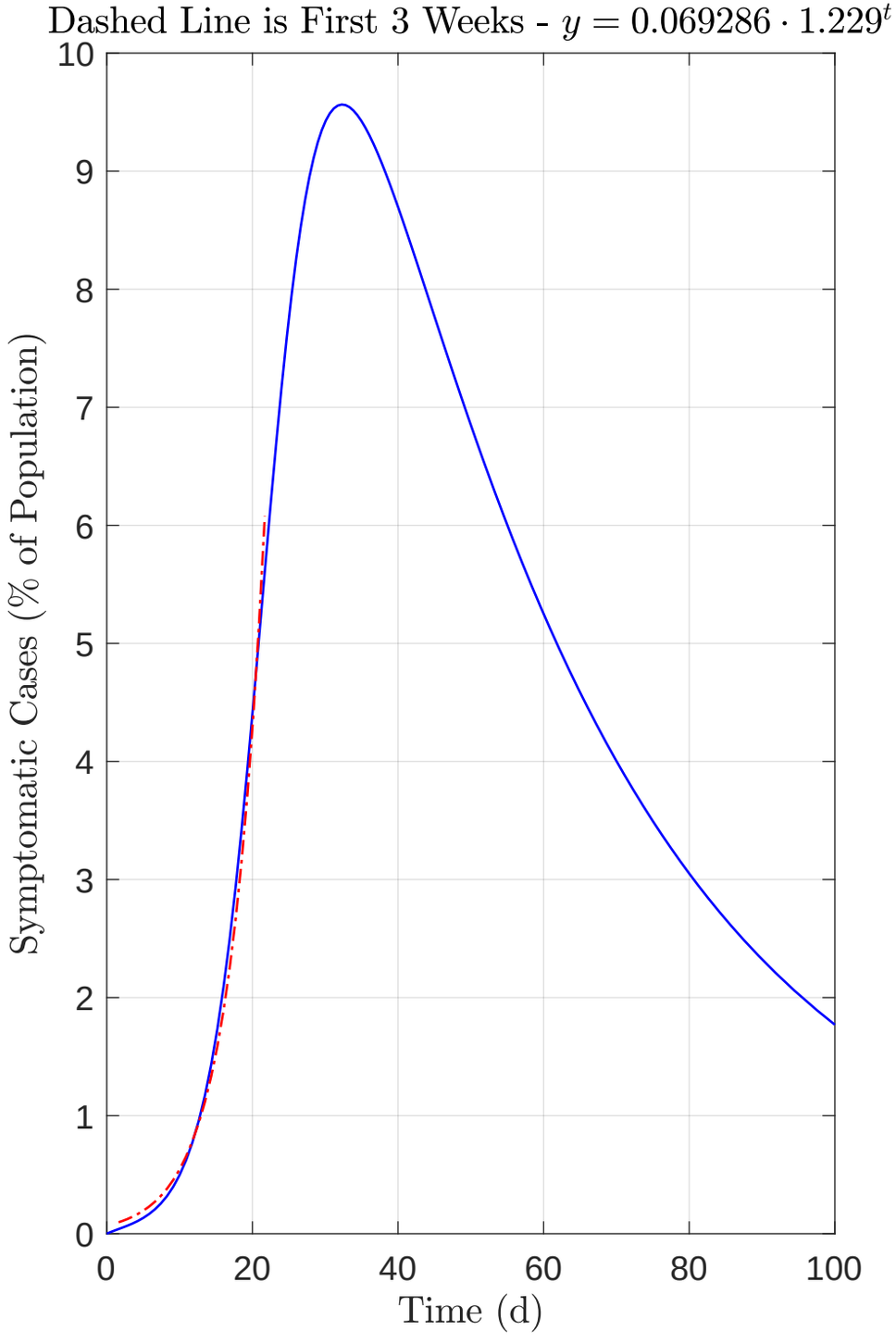
Dashed Line is First 3 Weeks - $y = 0.069286 \cdot 1.229^t$
Symptomatic Cases (% of Population)
Time (d)
0
1
2
3
4
5
6
7
8
9
10
0
20
40
60
80
100